

H. Khanpour · Ali N. Khorramian · S. Atashbar Tehrani

Parton Distribution Functions from QCD Analysis of HERA Combined Inclusive $e^\pm p$ Scattering Cross Section Data

Received: 14 October 2011 / Accepted: 22 November 2011 / Published online: 8 December 2011
© Springer-Verlag 2011

Abstract Utilizing very recent deep inelastic scattering measurements, a QCD analysis of proton structure function $F_2^p(x, Q^2)$ is presented. A wide range of the inclusive neutral-current deep-inelastic-scattering (NC DIS) data used in order to extract an updated set of parton distribution functions (PDFs). The HERA ‘combined’ data set on $\sigma_{r,NC}^\pm(x, Q^2)$ together with all available published data for heavy quarks $F_2^{c,b}(x, Q^2)$, longitudinal $F_L(x, Q^2)$ and also very recent reduced DIS cross section $\sigma_{r,NC}^\pm(x, Q^2)$ data from HERA experiments are the input in the present next-to-leading order (NLO) QCD analysis which determines a new set of parton distributions, called KKT11C. The extracted PDFs in the ‘fixed flavour number scheme’ (FFNS) are in very good agreement with the available theoretical models.

1 Introduction

Deep inelastic scattering (DIS) of leptons off nucleons is the basic process for our understanding of the structure of the nucleon. Very recently H1 and ZEUS collaborations at HERA have combined their inclusive deep inelastic cross sections measurements in neutral and charged current unpolarized $e^\pm p$ scattering into a single result [1]. This combined data set contains complete information on the DIS cross section, $\sigma_{r,NC}^\pm(x, Q^2)$. The kinematic range of the neutral current data is $0.045 \text{ GeV}^2 \leq Q^2 \leq 30,000 \text{ GeV}^2$ and $6 \times 10^{-7} \leq x \leq 0.65$, for values of inelasticity y between 0.005 and 0.95. HERA data provide crucial information on the small- x sea-quark and gluon parton distribution functions (PDFs). Analyses based on the NC DIS cross sections measured at HERA lead to precise sets of quark and gluon distributions in the proton together with the strong coupling constant, $\alpha_s(M_Z^2)$.

Presented by S. Atashbar Tehrani at LIGHTCONE 2011, 23–27 May, 2011, Dallas.

H. Khanpour · A. N. Khorramian
Physics Department, Semnan University, Semnan, Iran
E-mail: Hamzeh.Khanpour@nit.ac.ir

A. N. Khorramian
E-mail: Khorramiana@theory.ipm.ac.ir

H. Khanpour · A. N. Khorramian · S. Atashbar Tehrani (✉)
School of Particles and Accelerators, IPM (Institute for Studies in Theoretical Physics and Mathematics),
P.O.Box 19395-5531, Tehran, Iran
E-mail: Atashbar@ipm.ir

2 QCD Analysis

In the common $\overline{\text{MS}}$ factorization scheme the total structure function F_2^p as extracted from the DIS ep process can be, up to NLO, written as

$$\begin{aligned} F_2(x, Q^2) &= F_2^{\text{light}}(x, Q^2) + F_2^{\text{heavy}}(x, Q^2) \\ &= F_{2,\text{NS}}^+(x, Q^2) + F_{2,S}(x, Q^2) + F_2^{(c,b)}(x, Q^2, m_{c,b}^2), \end{aligned} \quad (1)$$

where $F_{i=2,L,3}^{\text{light}}$ is only the contributions of light partons (u, d, s , and g) to the total structure functions and the heavy quark contributions $F_{i=2,L,3}^{\text{heavy}} = F_i^h(x, Q^2, m_h^2)$ are the charm $F_i^c(x, Q^2, m_c^2)$ and bottom $F_i^b(x, Q^2, m_b^2)$ quark contributions. (Top quark contributions are negligible.) The basic formulae which are needed in our analysis, heavy quark thresholds and the structure of normalization of parton densities in singlet and non-singlet channels can be found for example in Refs. [2–8] in more detail.

The analysis is performed by taking into account the NLO corrections for the heavy flavor contributions in ‘fixed flavour number scheme’ (FFNS) [9, 10] where the heavy quarks ($h = c; b; t$) are considered as external particles which are not included among the partons in the colorless hadrons. We refer the reader to Refs. [4, 9, 10] for a detailed discussion of the FFN scheme. We use the exact solution of the DGLAP equation for the Mellin moments. The program QCD-PEGASUS [11] is used in order to perform all Q^2 -evolutions of the parton distributions.

2.1 Parametrization

PDFs are parameterized at the input scale $Q_0^2 = 2 \text{ GeV}^2$ by the following standard form

$$\begin{aligned} xu_v(x, Q_0^2) &= A_u x^{\alpha_u} (1-x)^{\beta_u} (1 + \gamma_u x^{\delta_u} + \eta_u x), \\ xd_v(x, Q_0^2) &= A_d x^{\alpha_d} (1-x)^{\beta_d} (1 + \gamma_d x^{\delta_d} + \eta_d x), \\ xS(x, Q_0^2) &= A_S x^{\alpha_S} (1-x)^{\beta_S} (1 + \gamma_S x^{\delta_S} + \eta_S x), \\ x\Delta(x, Q_0^2) &= A_\Delta x^{\alpha_\Delta} (1-x)^{\beta_S + \beta_\Delta} (1 + \gamma_\Delta x^{\delta_\Delta} + \eta_\Delta x), \\ xg(x, Q_0^2) &= A_g x^{\alpha_g} (1-x)^{\beta_g} (1 + \gamma_g x^{\delta_g} + \eta_g x), \end{aligned} \quad (2)$$

for the valence quark distributions xu_v and xd_v , the anti-quark distributions $xS = 2x(\bar{u} + \bar{d} + \bar{s})$ and $x\Delta = x(\bar{d} - \bar{u})$, and for gluon distribution xg .

For the anti-quark distribution $x\Delta$, we assume the power of $(1-x)$ to be $\beta_\Delta \rightarrow \beta_\Delta + \beta_S$ to avoid very small $x\Delta$ distribution at high x and to constrain \bar{u} and \bar{d} to be positive. For the gluon distribution xg , we need to have $x^{\delta_g=2}$ to give sufficient flexibility at low x and have a positive gluon distribution in this region. It is standard to assume that $s = \bar{s}$ and it is also common to use $s(x, Q_0^2) = \bar{s}(x, Q_0^2) = \frac{\kappa}{2}(\bar{u}(x, Q_0^2) + \bar{d}(x, Q_0^2))$ where in practice κ is a constant fixed in the range $\kappa = 0.4 - 0.5$.

The input PDFs listed in Eq. 2 are subject to the constraints $\int_0^1 u_v dx = 2$, $\int_0^1 d_v dx = 1$ and the sum rule

$$\int_0^1 x[u_v + d_v + S + g] dx = 1. \quad (3)$$

The parameters A_u, A_d and A_g were calculated using above constrains. This left us with a total of 28 independent fit parameters, including $\alpha_s(Q_0^2)$. We included in our final error analysis only those parameters that are actually sensitive to the input data set chosen. Using the data listed in Table 1 and our functional form of Eq. 2, only 13 such parameters, including $\alpha_s(Q_0^2)$, are included in our final error analysis.

2.2 Choice of Data Sets

The global fit reported in the present paper incorporates: the recent H1 and ZEUS combined measurement for inclusive $e^\pm p$ scattering cross sections [1] together with the most recent data from H1 collaboration [12]. The fixed target F_2^p data of NMC [13], BCDMS [14], E665 [15] and SLAC [16] and the data for F_2^d

Table 1 Experimental data sets included in the KKT11C global analysis

Experiment	Process	$[x_{min}, x_{max}]$	$[Q_{min}^2, Q_{max}^2]$	# of data points	$\Delta\mathcal{N}_n$ (%)	\mathcal{N}_n
NMC	$\mu p F_2$	[0.0045, 0.5]	[2.5, 65]	126 [13]	2	1.0023
NMC	$\mu d F_2$	[0.0045, 0.5]	[2.5, 65]	126 [13]	2	1.0023
NMC	$\mu n/\mu p$	[0.008, 0.675]	[2.23, 99.03]	156 [18]	0.15	0.9999
BCDMS	$\mu p F_2$	[0.07, 0.75]	[7.5, 230]	167 [14]	3	0.9928
BCDMS	$\mu d F_2$	[0.07, 0.75]	[8.75, 230]	155 [17]	3	0.9928
E665	$\mu p F_2$	[0.0037, 0.38726]	[2.046, 64.269]	53 [15]	1.85	1.0012
E665	$\mu d F_2$	[0.0037, 0.38726]	[2.046, 64.269]	53 [15]	1.85	1.0012
SLAC	$ep F_2$	[0.007, 0.65]	[2.01, 22.21]	53 [16]	2	1.0134
H1/ZEUS combined	$e^+ p, NC$	$[2.47 \times 10^{-5}, 0.65]$	[2, 30,000]	408 [1]	0.5	0.9998
H1/ZEUS combined	$e^- p, NC$	$[1.3 \times 10^{-3}, 0.65]$	[90, 30,000]	145 [1]	0.5	0.9998
H1 03–07	$e^\pm p, NC$	$[2.9 \times 10^{-5}, 0.01]$	[2, 120]	134 [12]	4	1.0007
H1	$ep F_2^c$	$[2.0 \times 10^{-4}, 0.05]$	[5, 2,000]	29 [19]	1.5	1.0000
H1	$ep F_2^c$	[0.005, 0.032]	[200, 650]	4 [21]	1.5	1.0014
H1	$ep F_2^c$	$[1.97 \times 10^{-4}, 0.05]$	[12, 60]	6 [22]	1.5	0.9995
H1	$ep F_2^c$	$[1.3 \times 10^{-4}, 0.00316]$	[3.5, 60]	10 [23]	1.5	0.9964
H1	$ep F_2^c$	$[8.0 \times 10^{-4}, 0.008]$	[12, 45]	9 [24]	1.5	0.9998
ZEUS	$ep F_2^c$	$[1.3 \times 10^{-4}, 0.00676]$	[4.2, 111.8]	5 [25]	1.8	0.9998
ZEUS	$ep F_2^c$	$[1.3 \times 10^{-4}, 0.02]$	[4, 130]	18 [26]	1.65	0.9999
ZEUS	$ep F_2^c$	$[3.0 \times 10^{-4}, 0.03]$	[2, 500]	31 [27]	2.2	0.9991
ZEUS	$ep F_2^c$	$[8.0 \times 10^{-4}, 0.03]$	[30, 1,000]	8 [20]	1.5	1.0002
H1	$ep F_2^b$	$[2.0 \times 10^{-4}, 0.05]$	[5, 2,000]	12 [19]	1.5	1.0000
H1	$ep F_2^b$	[0.005, 0.032]	[200, 650]	4 [21]	1.5	0.9997
H1	$ep F_2^b$	$[1.97 \times 10^{-4}, 0.05]$	[12, 60]	6 [22]	1.5	0.9999
ZEUS	$ep F_2^b$	$[8.0 \times 10^{-5}, 0.03]$	[30, 1000]	8 [20]	1.5	0.9997
H1	$ep F_2^c/F_2^p$	$[8.0 \times 10^{-4}, 0.008]$	[12, 45]	9 [24]	1.5	0.9996
H1/ZEUS	F_L	$[4.27 \times 10^{-5}, 0.0049]$	[2, 110]	65 [12,28–30]	–	1
FNAL E866/NuSea	DY, pd/pp	[0.026, 0.315]	54 (fixed)	30 [31,32]	0.6	0.9999
CHORUS	$\nu N x F_3$	[0.02, 0.65]	[2.052, 81.55]	50 [33]	2.1	1.0018
NuTeV	$\nu N x F_3$	[0.015, 0.75]	[3.162, 125.89]	64 [34]	2.1	1.0018
All data sets				1,944		

The fitted normalization \mathcal{N}_n of the data sets included in the global fit, together with the total normalization uncertainty, $\Delta\mathcal{N}_n$, for each data set n are also shown in the table. The details of corrections to data and the kinematic cuts applied are contained in the text

[13, 15, 17] and the structure function ratio F_2^d/F_2^p [18] all subject to the standard cuts $Q^2 \geq 2 \text{ GeV}^2$ and $W^2 = Q^2(\frac{1}{x} - 1) + m_p \geq 12.5 \text{ GeV}^2$. Furthermore we use the HERA measurements on the heavy flavour contribution to structure functions F_2^c , F_2^b and F_2^c/F_2^p of [19–27] and the direct HERA measurements of longitudinal protons structure function, F_L [12, 28–30]. The longitudinal structure function $F_L(x, Q^2)$ constrains the gluon positivity at small- x . The Drell–Yan dimuon pair production data of the E866/NuSea (fixed target) experiment [31, 32] also have been used. Finally, we include the $\nu(\bar{\nu})N x F_3$ data from CHORUS [33] and NuTeV [34]. A summary of the data sets used in this analysis are given in Table 1 and are ordered according to the type of process. The kinematical coverage of all the data sets included in KKT11C global analysis is summarized in this table. We provide in each case the number of data points and the ranges of the kinematical variables after kinematical cuts.

Above mentioned data sets contain 1944 data points from different experiments which lead to precise extractions of the PDFs. For the global fits a χ^2 minimization method is done using the program MINUIT [35]. More details on the experimental data selection, the corrections applied to the data and the statistical procedures used in the analysis see Ref. [4].

3 Quantitative Results

In the present article, we presented a comprehensive and updated NLO fit of DIS and related hard scattering data. The resulting parameters of the KKT11C fit including $\alpha_s(M_Z^2)$ together with the χ^2/dof value for PDFs fit are summarized in Table 2.

Table 2 Minimum values of χ^2 together with the input PDFs as parametrized in Eq. 2 referring to an input scale of $Q_0^2 = 2 \text{ GeV}^2$ determined from the KKT11C global analysis

	xu_v	xd_v	xS	$x\Delta$	xg
A	0.3868	0.6176	0.3562 ± 0.0015	8.7885 ± 2.2010	5.1597
α	0.4471 ± 0.0038	0.4278 ± 0.0081	-0.1740 ± 0.0020	1.3082 ± 0.1024	0.1015 ± 0.0115
β	3.5991 ± 0.0142	5.1495 ± 0.0625	7.7331 ± 0.0947	10.4027 ± 0.9236	8.0517 ± 0.3388
δ	0.1223	0.9819	0.0049	0.5620	2
γ	3.2695	-3.7539	0.4336	-7.9984	1.3235
η	21.2785	14.1453	12.4222	19.9294	-0.9380
χ^2/dof			$2004.379/1931 = 1.038$		

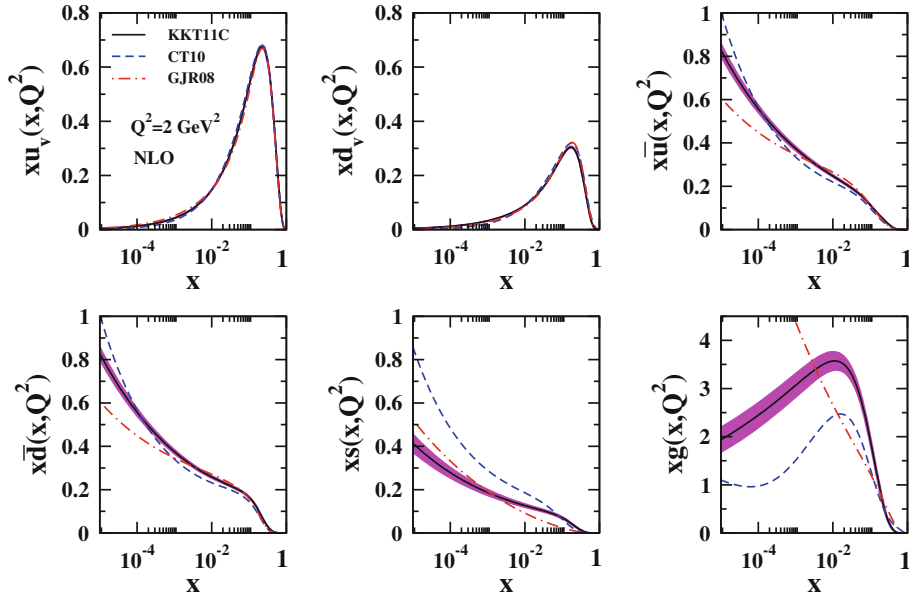


Fig. 1 The KKT11C parton distributions at input scale $Q_0^2 = 2 \text{ GeV}^2$ as a function of x in the NLO approximation. The GJR08 [3] and CT10 [36] added for comparison

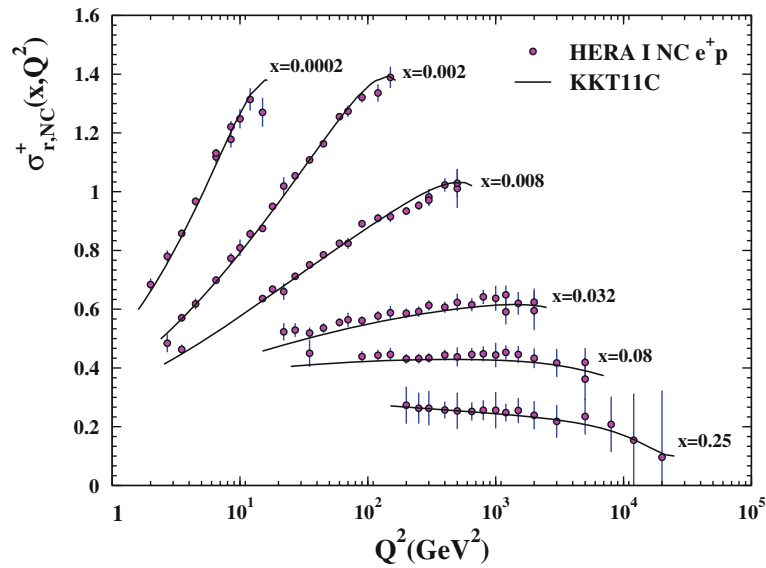


Fig. 2 A detailed comparison of our NLO ($\overline{\text{MS}}$) result for $\sigma_{r,NC}^+(x, Q^2)$ with a selection of HERA combined NC $e^+ p$ reduced cross section data [1]. The error bars indicate the total experimental uncertainty

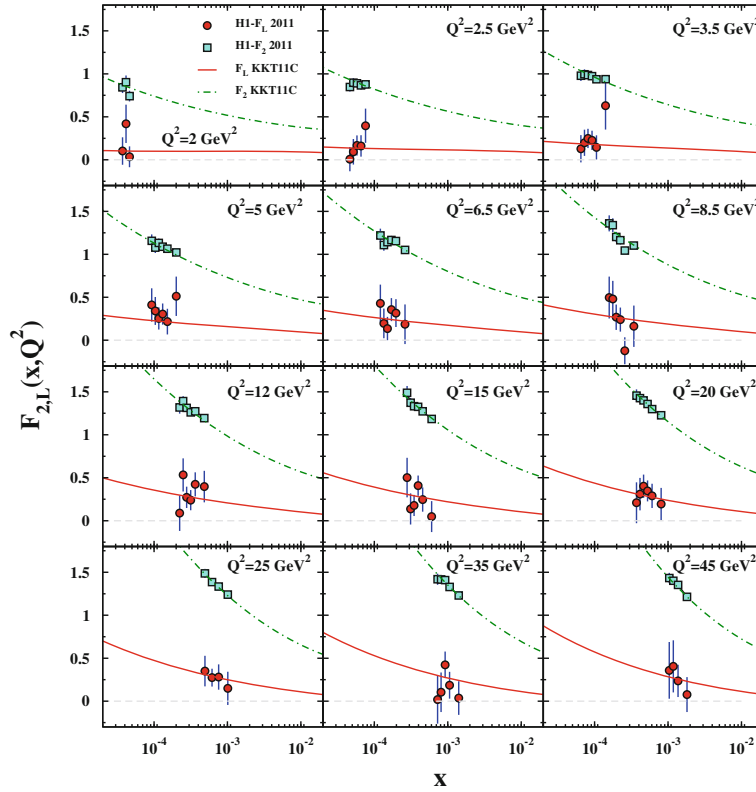


Fig. 3 Our results for the proton structure function, $F_2(x, Q^2)$ and $F_L(x, Q^2)$, at NLO in comparison with recent H1 data [12]. The full error bars include the statistical and systematic uncertainties added in quadrature

The resulting PDFs from present QCD analysis are shown in Fig. 1 where they are compared to GJR08 [3] and CT10 [36]. A detailed comparison of our NLO ($\overline{\text{MS}}$) result for $\sigma_{r,NC}^+(x, Q^2)$ with a selection of HERA combined data [1] is shown in Fig. 2.

Representative comparisons of our results with the most recent HERA-H1 data [12] on the structure function of the proton, $F_2(x, Q^2)$ and $F_L(x, Q^2)$, are presented in Fig. 3. The curves represent the results of the KKT11C fit in the FFN scheme for the structure functions F_2 and F_L .

It should be more accurate to determine α_s from PDF fits of deep-inelastic QCD analysis. We include $\alpha_s(Q_0^2)$ as a free parameter in our fits thus the running coupling constant is determined in our analysis together with the parton distributions of the nucleon. The strong coupling constant obtained from our standard NLO analysis is $\alpha_s(M_Z^2) = 0.1165 \pm 0.0013$.

A FORTRAN package (grid) containing our standard NLO ($\overline{\text{MS}}$) PDFs can be obtained from <http://particles.ipm.ir/links/QCD.htm> [37].

Acknowledgments We are especially grateful to F.Olness for many fruitful suggestions and critical remarks. A.N.K thanks the CERN TH-PH division for the hospitality where a portion of this work was performed.

References

1. Aaron, F.D., et al., H1 and ZEUS Collaboration: Combined measurement and QCD analysis of the inclusive $e\pm p$ scattering cross sections at HERA. JHEP **1001**, 109 (2010). arXiv:0911.0884 [hep-ex]
2. Martin, A.D., Stirling, W.J., Thorne, R.S., Watt, G.: Parton distributions for the LHC. Eur. Phys. J. C **63**, 189 (2009). arXiv:0901.0002 [hep-ph]
3. Gluck, M., Jimenez-Delgado, P., Reya, E.: Dynamical parton distributions of the nucleon and very small- x physics. Eur. Phys. J. C **53**, 355 (2008). arXiv:0709.0614 [hep-ph]
4. Khanpour, H., Khorrarnian, A.N., Atashbar Tehrani, S.: Next-to-leading order parton distributions in fixed flavour factorization scheme from recent deep-inelastic-scattering data. Phys. Rev. D (2012, to appear)

5. Khorramian, A.N., Khanpour, H., Tehrani, S.A.: Nonsinglet parton distribution functions from the precise next-to-next-to-next-to leading order QCD fit. *Phys. Rev. D* **81**, 014013 (2010). arXiv:0909.2665 [hep-ph]
6. Khanpour, H., Khorramian, A.N., Atashbar Tehrani, S., Mirjalili, A.: Determination of valance quark distributions in higher order of perturbative QCD. *Acta Phys. Polon. B* **40**, 2971 (2009)
7. Khorramian, A.N., Tehrani, S.A.: NNLO QCD contributions to the flavour non-singlet sector of $F_2(x, Q^2)$. *Phys. Rev. D* **78**, 074019 (2008). arXiv:0805.3063 [hep-ph]
8. Atashbar Tehrani, S., Khorramian, A.N.: The Jacobi Polynomials QCD analysis for the polarized structure function. *JHEP* **0707**, 048 (2007). arXiv:0705.2647 [hep-ph]
9. Riemersma, S., Smith, J., van Neerven, W.L.: Rates for inclusive deep inelastic electroproduction of charm quarks at HERA. *Phys. Lett. B* **347**, 143 (1995). arXiv:hep-ph/9411431
10. Laenen, E., Riemersma, S., Smith, J., van Neerven, W.L.: Complete O (α_s) corrections to heavy flavour structure functions in electroproduction. *Nucl. Phys. B* **392**, 162 (1993)
11. Vogt, A.: Efficient evolution of unpolarized and polarized parton distributions with QCD-PEGASUS. *Comput. Phys. Commun.* **170**, 65 (2005). arXiv:hep-ph/0408244
12. Collaboration, H.: Measurement of the inclusive $e\pm p$ scattering cross section at high inelasticity y and of the structure function F_L . *Eur. Phys. J. C* **71**, 1579 (2011). arXiv:1012.4355 [hep-ex]
13. Arneodo, M., et al., New Muon Collaboration: Measurement of the proton and deuteron structure functions, $F_2(p)$ and $F_2(d)$, and of the ratio $\sigma(L)/\sigma(T)$. *Nucl. Phys. B* **483**, 3 (1997). arXiv:hep-ph/9610231
14. Benvenuti, A.C., et al., BCDMS Collaboration: A high statistics measurement of the proton structure functions $F_2(x, Q^2)$ and R from deep inelastic muon scattering at high Q^2 . *Phys. Lett. B* **223**, 485 (1989)
15. Adams, M.R., et al., E665 Collaboration: Proton and deuteron structure functions in muon scattering at 470-GeV. *Phys. Rev. D* **54**, 3006 (1996)
16. Whitlow, L.W., Riordan, E.M., Dasu, S., Rock, S., Bodek, A.: Precise measurements of the proton and deuteron structure functions from a global analysis of the SLAC deep inelastic electron scattering cross-sections. *Phys. Lett. B* **282**, 475 (1992)
17. Benvenuti, A.C., et al., BCDMS Collaboration: A high statistics measurement of the deuteron structure functions $F_2(x, Q^2)$ and R from deep inelastic muon scattering at high Q^2 . *Phys. Lett. B* **237**, 592 (1990)
18. Arneodo, M., et al., New Muon Collaboration: Accurate measurement of $F_2(d)/F_2(p)$ and $R(d)-R(p)$. *Nucl. Phys. B* **487**, 3 (1997). arXiv:hep-ex/9611022
19. Aaron, F.D., et al., H1 Collaboration: Measurement of the charm and beauty structure functions using the H1 vertex detector at HERA. *Eur. Phys. J. C* **65**, 89 (2010). arXiv:0907.2643 [hep-ex]
20. Chekanov, S., et al., ZEUS Collaboration: Measurement of charm and beauty production in deep inelastic ep scattering from decays into muons at HERA. *Eur. Phys. J. C* **65**, 65 (2010). arXiv:0904.3487 [hep-ex]
21. Aktas, A., et al., H1 Collaboration: Measurement of $F_2(c\bar{c})$ and $F_2(b\bar{b})$ at high Q^2 using the H1 vertex detector at HERA. *Eur. Phys. J. C* **40**, 349 (2005). arXiv:hep-ex/0411046
22. Aktas, A., et al., H1 Collaboration: Measurement of $F_2(c \text{ anti-}c)$ and $F_2(b \text{ anti-}b)$ at low Q^2 and x using the H1 vertex detector at HERA. *Eur. Phys. J. C* **45**, 23 (2006). arXiv:hep-ex/0507081
23. Adloff, C., et al., H1 Collaboration: Measurement of D^{*+} - meson production and $F_2(c)$ in deep inelastic scattering at HERA. *Phys. Lett. B* **528**, 199 (2002). arXiv:hep-ex/0108039
24. Adloff, C., et al., H1 Collaboration: Inclusive D_0 and D^{*+} - production in neutral current deep inelastic e p scattering at HERA. *Z. Phys. C* **72**, 593 (1996). arXiv:hep-ex/9607012
25. Chekanov, S., et al., ZEUS Collaboration: Measurement of D mesons production in deep inelastic scattering at HERA. *JHEP* **0707**, 074 (2007). arXiv:0704.3562 [hep-ex]
26. Breitweg, J., et al., ZEUS Collaboration: Measurement of D^{*+} - production and the charm contribution to F_2 in deep inelastic scattering at HERA. *Eur. Phys. J. C* **12**, 35 (2000). arXiv:hep-ex/9908012
27. Chekanov, S., et al., ZEUS Collaboration: Measurement of D^{*+} - production in deep inelastic $e^+ p$ scattering at HERA. *Phys. Rev. D* **69**, 012004 (2004). arXiv:hep-ex/0308068
28. Adloff, C., et al., H1 Collaboration: Deep-inelastic inclusive e p scattering at low x and a determination of α_s . *Eur. Phys. J. C* **21**, 33 (2001). arXiv:hep-ex/0012053
29. Chekanov, S., et al., ZEUS Collaboration: Measurement of the Longitudinal Proton Structure Function at HERA. *Phys. Lett. B* **682**, 8 (2009). arXiv:0904.1092 [hep-ex]
30. Aaron, F.D., et al., H1 Collaboration: Measurement of the Proton Structure Function F_L at Low x . *Phys. Lett. B* **665**, 139 (2008). arXiv:0805.2809 [hep-ex]
31. Towell, R.S., et al., FNAL E866/NuSea Collaboration: Improved measurement of the anti-d/anti-u asymmetry in the nucleon sea. *Phys. Rev. D* **64**, 052002 (2001). arXiv:hep-ex/0103030
32. Webb, J.C., et al., NuSea Collaboration: Absolute Drell-Yan dimuon cross sections in 800-GeV/c p p and p d collisions. arXiv: hep-ex/0302019
33. Onengut, G., et al., CHORUS Collaboration: Measurement of nucleon structure functions in neutrino scattering. *Phys. Lett. B* **632**, 65 (2006)
34. Tzanov, M., et al., NuTeV Collaboration: Precise measurement of neutrino and anti-neutrino differential cross sections. *Phys. Rev. D* **74**, 012008 (2006). arXiv:hep-ex/0509010
35. James, F.: CERN Program Library, Long Writeup D506 (MINUIT)
36. Lai, H.L., Guzzi, M., Huston, J., Li, Z., Nadolsky, P.M., Pumplin, J., Yuan, C.P.: New parton distributions for collider physics. *Phys. Rev. D* **82**, 074024 (2010). arXiv:1007.2241 [hep-ph]
37. Program summary <http://particles.ipm.ir/links/QCD.htm>